CrossMark

ORIGINAL ARTICLE

A Kriging and Stochastic Collocation ensemble for uncertainty quantification in engineering applications

A. Kaintura[1] · D. Spina[1] · I. Couckuyt[1] · L. Knockaert[1] · W. Bogaerts [2] · T. Dhaene[1,2]

Abstract We propose a new surrogate modeling approach by combining two non-intrusive techniques: Kriging and Stochastic Collocation. The proposed method relies on building a sufficiently accurate Stochastic Collocation model which acts as a basis to construct a Kriging model on the residuals, to combine the accuracy and efficiency of Stochastic Collocation methods in describing stochastic quantities with the flexibility and modeling power of Kriging-based approaches. We investigate and compare performance of the proposed approach with state-of-art techniques over benchmark problems and practical engineering examples on various experimental designs.

Keywords Surrogate modeling · Stochastic Collocation · Kriging · Uncertainty quantification

1 Introduction

The development of Computer Aided Design and Engineering (CAD / CAE) software in the past decades has made it possible to analyze and achieve efficient designs for complex engineering problems. However, accurate physics-based simulation programs can be computational very expensive, which is a limiting factor for the application to complex engineering applications. Surrogate models [1] are generally adopted as a reliable approach to study computational intensive problems. Surrogate models approximate the input–output behavior of complex physical systems and, once built with sufficient accuracy, can be evaluated very efficiently. Thus, they can be easily employed to perform any routine tasks in optimization, sensitivity analysis (SA), and uncertainty quantification (UQ) [2–5].

The application of these surrogate models in UQ is becoming increasingly popular [4, 6]. Physical systems are often affected by uncertainties present in many physical parameters. To simulate the behavior of a physical system, exact values of these input parameters are required. For instance, to simulate the behavior of a cantilever beam which is acted upon by various loads requires exact knowledge of the beam material, geometrical properties, and acting loads. These parameters may vary due to the manufacturing tolerances, measurement errors, or due to the natural variability and, hence, are random in nature. These uncertainties which are present due to the variability in the inputs parameters (or models) are characterized as aleatory uncertainty, which are irreducible in nature. Therefore, to simulate the behavior of a physical system, it becomes necessary to take these uncertainties into account. These uncertainties need to be identified, included, and propagated through the model for a reliable realization of the response quantities.

Aleatory uncertainties can be quantified by a probabilistic framework, where uncertain input parameters are represented as random variables, and, therefore, characterized by their joint probability distribution. Thereafter, a surrogate model can be used to propagate uncertainty from inputs to outputs. Various surrogate models are surveyed in [3, 7]. Here, we particularly focus on non-intrusive techniques for constructing surrogate models for UQ purposes. Such techniques do not require modification of the existing deterministic solvers to provide relevant statistical information

✉ A. Kaintura
   arun.kaintura@ugent.be

1   IDLab, Department of Information Technology (INTEC), Ghent University–imec, Technologiepark–Zwijnaarde 15, 9052 Ghent, Belgium

2   Photonics Research Group, Department of Information Technology, Center for Nano and Biophotonics, Ghent University– imec, 9050 Ghent, Belgium

Springer

about the problem under study. Thus, a surrogate model is built on an input vector and the corresponding output response(s).

Various surrogate models exists in the literature with interesting statistical properties: for example Kriging (Kr) [8, 9], Polynomial Chaos (PC) [10, 11], Stochastic Collocation (SC) [12, 13], Polynomial Chaos-Based Kriging (PCK) [14], and Support Vector Regression (SVR) [15].

Kr is a surrogate model based on Gaussian process regression. Its capability to predict multi-dimensional and non-linear responses from scattered data gives it growing popularity. For example, in [16, 17], efficient and robust Kr schemes suitable to various realistic engineering problems have been presented.

The PC expansion instead approximates a stochastic process as a series of orthogonal polynomials with respect to the distributions of the input random variables [10, 11]. Several PC-based techniques have been developed in the recent years. The multi-element generalized PC method (ME-gPC) was introduced to address discontinuities in the random space by decomposing the random inputs space into disjoint random elements [18, 19]. Recently, a multi-element method was proposed in [20, 21], which discretizes the random space using a simplex tessellation of sampling points. Multi-resolution schemes have been proposed in [22, 23], representing the random variables in terms of polynomial multi-wavelets. Recently, the PC expansion has also been combined with Model Order Reduction techniques [24, 25], to study system described by a large set of equations. In [26], a sparse PC expansion was introduced to efficiently detect significant coefficients of PC expansion based on the least angle regression algorithm, while a weighted ℓ_1-minimization approach was proposed in [27] to obtain sparse PC expansions suitable to solve differential equations with high-dimensional random inputs.

SC methods [28] are stochastic expansion techniques based on interpolations built over a pre-determined set of nodes in a stochastic space. The multi-dimensional interpolation is constructed through either full tensor product of one-dimensional (1D) interpolation rule or by more efficient schemes, like sparse grid interpolation method [6, 12, 29], dimension adaptive [6, 30, 31], and hierarchical approaches. In [32, 33], an adaptive piecewise linear hierarchical sparse grid approximation was used [34, 35].

In this paper, we focus on Kr and SC approaches and their application in UQ. While the application of Kr approaches and SC methods in UQ has been investigated in the past and discussed in various contributions, e.g., [4, 6, 9, 36], the modeling technique proposed in this paper is a unique combination of SC and Kr methods. It is a non-intrusive technique and can be used in all domains where SC and Kr approaches have applications. It is based on the first building an SC model to capture the global behavior of

the quantity under study (system response) using minimum number of samples possible. We do not aim to completely describe the system response over the stochastic space, but only to capture its trend (global trend of the response). Next, a Kr model is built to capture the variations between the trend (output of the SC model) and the system response (i.e., local neighborhood features such as extreme values). Hence, the proposed modeling approach is based on two different phases: first, the global behavior and then the local variations are modeled by means of SC and Kr techniques, respectively. The proposed ensemble of SC and Kr takes advantage of the unique features of the two modeling techniques employed and allows to overcome their limitations, as described in the following sections.

This paper is structured as follows. First, an overview of the properties of SC and Kr methods is given in Sects. 2 and 3, respectively. The new modeling technique is described in Sect. 4, while validation is performed in Sect. 5 by means of suitable numerical examples. The conclusions are summed up in Sect. 6.

2 Stochastic Collocation

SC methods are based on interpolation schemes to compute stochastic quantities. The interpolation is constructed by repeatedly solving (sampling) the problem at a pre-determined set of nodes in the stochastic space (also referred as collocation points) [12]. Various types of interpolation schemes can be adopted such as piecewise linear, Lagrange [6, 11, 31, 37]. However, the key issue of this approach is the selection of nodes, such that with a minimal number of nodes, a good approximation can be obtained. In case of one random variable, a stochastic process **Y** is expressed as a function of the interpolation basis:

$$\mathbf{U}(\xi) = \sum_{i=1}^{N} \mathbf{Y}(\xi_i) L_i(\xi) \tag{1}$$

where ξ is a random variable, N is the number of unique collocation points, $\mathbf{Y}(\xi_i)$ is a system response matrix, and $\{L_i(\xi), i = 1, \ldots, N\}$ are the interpolation basis functions. Please note that the explicit dependency of **Y** from the time (or frequency) is omitted in Eq. (1) and in the rest of the paper, for ease of notation. In this contribution, we adopt Lagrange interpolating basis functions which for the univariate case, which can be written as follows:

$$L_j(\xi) = \prod_{i=1, i \neq j}^{N} \frac{\xi - \xi_i}{\xi_j - \xi_i}. \tag{2}$$

By construction, the value of the jth Lagrange basis is equal to 1 for $\xi = \xi_j$ and equal to 0 for $\xi = \xi_i$ in Eq. (1): the SC model is equal to the function values at the collocation

points. Moreover, SC heavily relies on the choice of collocation points which minimizes the maximum interpolation error [31], such as Chebyshev and Gauss points. In a multi-dimensional problem, these one-dimensional nodes are extended to a multi-dimensional grid by means of the tensor product. Therefore, in a d-dimensional space, the interpolation function can be expressed as follows:

$$
\begin{aligned}
\mathbf{Y}(\xi) &= \mathbf{U}^{k_1} \otimes \cdots \otimes \mathbf{U}^{k_d} \\
&= \sum_{i_1=1}^{N_{k_1}} \cdots \sum_{i_d=1}^{N_{k_d}} \mathbf{Y}(\xi_{i_1}^{k_1}, \ldots, \xi_{i_d}^{k_d})(L_{i_1}^{k_1} \otimes \cdots \otimes L_{i_d}^{k_d})
\end{aligned}
\tag{3}
$$

where $\mathbf{U}^{k_1}$ represents the interpolation scheme in the form (1) with respect to the random variable ξ_j and ξ_i^k is the ith node in the kth direction. A full tensor product has $N_{k_1} \times \cdots \times N_{k_d}$ nodes. Clearly, the data requirements increase rapidly with respect to the number of stochastic parameters. Alternatively, the adoption of sparse grids based on the Smolyak algorithm [6, 12, 29] is an efficient approach to reduce the required number of nodes while preserving the interpolation properties: the desired interpolant is built as a linear combination of tensor products. More details about Smolyak sparse grid are given in Appendix 1.

Hence, to build an SC model, it is crucial to choose the interpolation scheme and the nodes selection strategy. As remarked above, in this contribution, we will adopt the Lagrange interpolation and a Smolyak grid based on the Clenshaw Curtis and Gauss Legendre rules to choose the collocation points. Clenshaw Curtis choice is particularly efficient, since the resulting sparse grid is nested: if additional nodes are required to accurately model the system response, the nodes already computed are used in the new sparse grid. Once an SC model has been built, stochastic moments can be computed very efficiently, for example, via numerical integration or MC analysis of the obtained SC model. A more detailed discussion on SC methods is given in [11, 12, 37].

3 Kriging

Kr is a popular surrogate modeling technique also known as Gaussian process modeling and has proven to be useful in various engineering applications such as design and optimization [2, 8]. This section discusses the basic theory of Kr required for the formulation of the proposed method.

We consider a sample size of N with $\{X = \mathbf{x}_i, i = 1, \ldots, N\}$ as observations in a d-dimensional space and the corresponding output response as $\{y = y_i, i = 1, \ldots, N\}$. A Kr model assumes a deterministic response as a realization of a Gaussian process $\mathbf{Y}(\mathbf{x})$ and is expressed with a regression part $\mathbf{f}(\mathbf{x})$ and a stochastic process $\mathbf{Z}(\mathbf{x})$ through the residuals:

$$
\mathbf{Y}(\mathbf{x}) = \mathbf{f}(\mathbf{x}) + \mathbf{Z}(\mathbf{x}).
\tag{4}
$$

In practice, based on the choice of the regression function used in Eq. (4), Kr can be classified by different terms, for example with $\mathbf{f}(\mathbf{x}) = 0$ and $\mathbf{f}(\mathbf{x}) = \alpha_0$, the modeling process is referred to as simple or ordinary Kr, respectively. In general, the Kr regression function can be of any form, such as a combination of polynomials or basis functions. Kr with such a trend function, i.e., $\mathbf{f}(\mathbf{x}) = \boldsymbol{\alpha}^{\mathbf{T}}\mathbf{b}(\mathbf{x})$, is classified as universal Kr. It captures the major trend or the largest variations in the data. In particular, $\{\alpha_1, \ldots, \alpha_p\}$ are the regression coefficients for the basis functions $\{b(\mathbf{x}) = b_i(\mathbf{x}), i = 1, \ldots, p\}$ and $\mathbf{Z}(\mathbf{x})$ is a stationary Gaussian process with the properties $\mathbf{E}(\mathbf{Z}(\mathbf{x})) = 0$, $Var(\mathbf{Z}(\mathbf{x})) = \sigma^2$, $Cov(\mathbf{Z}(\mathbf{x}_i), \mathbf{Z}(\mathbf{x}_j)) = \sigma^2 \mathbf{R}(\mathbf{x}_i, \mathbf{x}_j)$. The symbol σ^2 is the process variance and $\mathbf{R}(\mathbf{x}_i, \mathbf{x}_j)$ is a correlation function between two sampled points which is parameterized by a hyperparameter vector θ. Note that, at any unknown point $\mathbf{x}$ in the design space, a Kr model estimates a predictive Gaussian distribution with mean (output response) and variance (uncertainty) [38]. Now, building a reasonably accurate model requires an appropriate choice of the correlation function and its hyperparameters. Various correlation functions can be found in the literature [8], such as exponential, Matérn, and Gaussian correlation functions. In this paper, examples from different domains have been used to study the performance of the proposed technique. Since it would be difficult to choose the best covariance function for each specific case, to maintain coherency, we have used the most popular and well−known Gaussian function in all the numerical examples shown in the paper, which is formulated as:

$$
R(\mathbf{x}_i, \mathbf{x}_j) = exp\left(-\sum_{k=1}^{d} \theta_k |\mathbf{x}_i^k - \mathbf{x}_j^k|^2\right)
\tag{5}
$$

where $\mathbf{x}_i$ and $\mathbf{x}_j$ are two sampled points in the input space X. The hyperparameters are obtained by Maximum-Likelihood Estimation (MLE) [38].

Finally, to build accurate Kr models, it is also important to choose the training samples well preferably by space filling criteria [39]. A Latin Hypercube Design (LHD) is often used to build Kr models. Moreover, various systematic sampling schemes exist to improve the Kr approximation, such as based on maximizing the variance [40], expected improvement which is purely used for optimization [41]. For a detailed derivation of the Kr method, readers may refer to [38].

4 Stochastic Collocation and Kriging ensemble

4.1 Introduction

Even if the two methods described in Sects. 2 and 3 are both interpolation-based, they have quite different characteristics. Let us consider SC models in the form of Eq. (3), which are based on a tensor product of the one-dimensional interpolation functions for each dimension. Now, the value of such a SC model in a specific point of the stochastic space depends on the value of the interpolant built for each dimension. Hence, the nodes selection strategy for the interpolation in each dimension is chosen from a node distribution which guarantees a good quality of the interpolation (such as the extrema of the Chebyshev polynomials) [6]. As a result, the value of the stochastic process under study in each node contributes to the value of the SC model in each point of the stochastic space. Now, SC models which take advantage of the Smolyak sparse grid construction are based on the same principle. However, only a subset of the total nodes resulting from a full tensor product of each one-dimensional interpolant functions is used, see Appendix 1. These sub-sets are based on a constraint on the maximum order of the (overall) interpolating polynomial function.

Instead, Kr-based modeling approaches interpolate based on the underlying covariance structure. Once the covariance function is estimated, a Kr model can predict the values of the system response at new points in the sample space. To estimate the covariance function, it is well known that space filling sampling is an advantage [42, 43].

Hence, SC and Kr-based methods have different properties: SC modeling approaches are simple to implement, stable, and in general can conveniently handle non-linear or complex problems. However, they are based on a predetermined set of nodes which depends on the maximum degree chosen for the (overall) interpolating polynomial function, see Eq. (17). For instance, the node requirements for SC models based on a specific sampling strategy (Smolyak sparse grid based on the Clenshaw–Curtis rule) for different number of random parameters are shown in Table 1. It can be seen that the number of nodes required to build a sparse grid increases drastically with respect to the number of parameters considered. Whereas, Kr can accept irregularly filled data and interpolates based on the correlation between known data for unknown values in the sample space: it can easily capture the local characteristics of the underlying function.

In this contribution, we propose a combined SC and Kr framework (SCK), which overcomes the limitations of both approaches. The core of the proposed method is building an SC model based on a low-degree polynomial interpolant. Such an SC model will not be accurate enough to describe the variations of the stochastic process under study over the entire design space, but is able to capture the global trends in such process. Furthermore, since the degree of the interpolant is directly related to the node requirements, the total number of collocation points used to build such SC model is relatively limited. Note that SC methods are particularly suitable to fill this role, since the value of the SC model in each point of the stochastic space depends on the value of the interpolant built for each dimension.

Next, a Kr model is built to capture the deviations of the stochastic process from its global trend: Kr is used to describe the local variations of the stochastic process under study. Note that the Kr model can be built on the samples generated from any experimental design: a pre-determined set of samples is not required. Furthermore, various systematic sampling schemes can be adopted (Sect. 3) to improve Kr approximation. Hence, the proposed method combines the accuracy of SC methods in describing stochastic quantities with the flexibility and modeling power of Kr.

In the PCK approach (which is a particular case of universal Kr), the mean function of Kr is replaced by a set of an orthogonal polynomials. Note that these polynomials are obtained through PC using the same set of data which is used to construct Kriging model, whereas it is different in SCK where SC nodes are not used to construct Kriging model (as the residuals there would be zero). However, as a result, the Kr model in the PCK formulation can be computationally complex. In particular, when number of dimensions increases, the corresponding number of PC basis function increases as well, which may lead to an expensive model evaluation, as shown in the numerical examples, Sect. 5.3.

Now, using SC basis functions (Lagrange) as a mean function for Kr will have the same drawback as the PCK approach. The proposed approach overcomes such

Table 1 Number of nodes required for construction of the Smolyak grid based on Clenshaw–Curtis rule

Two dimensions								
Level	1	2	3	4	5	6	7	8
No. of nodes	5	13	29	65	145	321	705	1537
Eight dimensions								
Level	1	2	3	4	5	6	7	8
No. of nodes	17	145	849	3937	15713	56737	190881	609025

problems using a different approach with respect to universal Kr: the SC is used to model the global behavior (trend) of the system response, while Kr models the variations between the trend and the system response and modeled separately.

Not only the proposed modeling approach takes full advantage of capability of SC of adopting collocation points able to minimize the interpolation error, but the proposed technique is particularly suited for UQ analysis where multiple model evaluations are required to estimate complex stochastic quantities like the probability distribution function (PDF) and cumulative distribution function (CDF), since the SC and Kr part of the SCK model can be evaluated separately and in parallel. Furthermore, simple stochastic moments can be efficiently computed, see Sect. 4.3, even analytically.

4.2 Conceptual formulation

We use the same notations as described for the SC and Kr formulation in this section as well. We denote $\mathbf{Y^{SC}}(\xi)$ and $\mathbf{Y^{Krig}}(\mathbf{x})$ as the SC and Kr computational model responses, respectively.

The whole process is conceived in two steps. In the first step, a sufficiently reliable SC model $\mathbf{Y^{SC}}(\xi)$ (Eq. 1) is built on pre-defined nodes of size $N\left\{\xi^{SC} = \xi_i, i = 1, \ldots, N\right\}$ in an input space Ω using a sparse grid construction. A better accuracy could be achieved by increasing the level of the sparse grid which significantly increases the number of nodes as well, but this is not the objective here.

In the second step, M samples $\left\{\xi^K = \xi_j, j = 1, \ldots, M\right\}$ are generated using space filling methods. Subsequently, the response of the SC model over these samples is obtained $\left\{\mathbf{Y^{SC}}(\xi_j), i = 1, \ldots, M\right\}$.

Next, we compute the SC model error over the M samples ξ^K as $\Delta\mathbf{Y} = \mathbf{Y^{Exact}}(\xi^K) - \mathbf{Y^{SC}}(\xi^K)$, where $\mathbf{Y^{Exact}}(\xi^K)$ is the output response on the samples ξ^K. Taking ξ^K as the input data and $\Delta\mathbf{Y}$ as the corresponding response, a Kr

model $\mathbf{Y^{Krig}}(\xi)$ is then built over the sample space. Finally, the response on any new sampled point ξ in the input space is computed as sum of the SC and Kr models explicitly expressed as follows:

$$\mathbf{Y}^{SCK}(\xi) = \mathbf{Y}^{SC}(\xi) + \mathbf{Y}^{Krig}(\xi) \tag{6}$$

$$= \sum_{i=1}^{N} \mathbf{Y}(\xi)L_i(\xi) + \boldsymbol{\alpha}^{\mathbf{T}}\mathbf{b}(\xi) + \mathbf{Z}(\xi). \tag{7}$$

It is important to note that the ξ^K samples must be different from the ξ^{SC} samples, since, by construction, the SC model is equal to the system response on the nodes, leading to $\Delta\mathbf{Y} = 0$. The sampling strategy and the flowchart of the proposed SCK method are shown in Figs. 1 and 2, respectively.

4.3 SCK-based uncertainty quantification

SC and Kr are popular approaches to approximate stochastic behaviors in UQ problems (see Sects. 2 and 3). A typical UQ problem involves determination of statistical moments of the output quantities of interest with respect to the joint input distribution. To compute these moments, integrals have to be solved such as for the mean, i.e., Eq. (8) and variance (σ^2), i.e., Eq. (9). The standard approach for UQ is the Monte Carlo (MC) method, which is accurate and robust, but not computationally efficient, due to the high number of required simulations. In case of SC, statistical moments can be computed as described in Sect. 2, namely via analytical formulas (when possible) or numerical integration techniques [11]. Note that Kr mean and variance can be computed analytically too via MC analysis based on the computed Kr model:

$$\mu = \int_{\Omega} \mathbf{Y}(\xi)W(\xi)d\xi \tag{8}$$

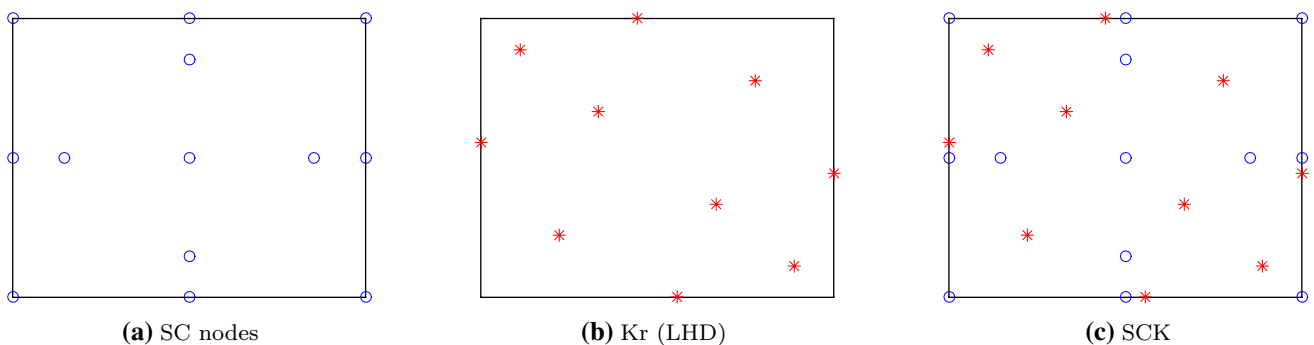$$\sigma^2 = \int_{\Omega} (\mathbf{Y}(\xi) - \mu)^2 W(\xi)d\xi. \tag{9}$$

(a) SC nodes   **(b)** Kr (LHD)   **(c)** SCK

Fig. 1 Two-dimensional case, **a** SC nodes (13 nodes) based on Clenshaw Curtis, **b** LHD of 10 samples for Kr, and **c** final combined 23 samples for SCK
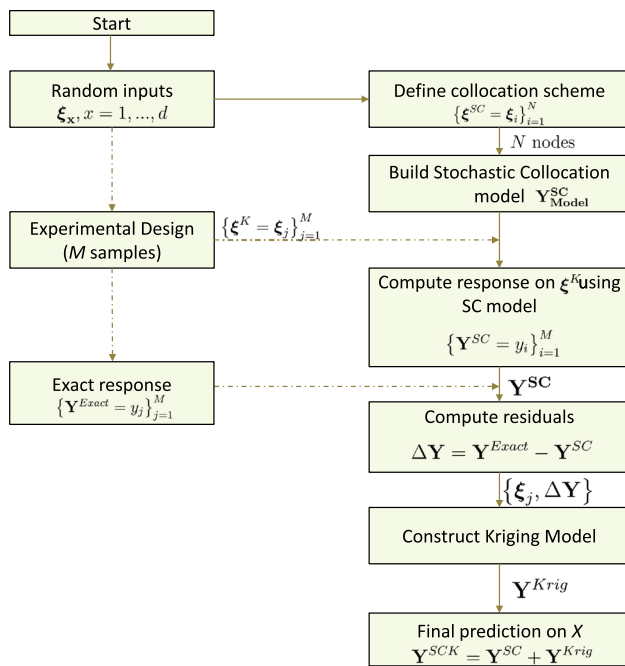
Fig. 2 Description of the proposed ensemble modeling strategy (SCK)

Now, the mean of any stochastic process $\mathbf{Y}$ described via an SCK model can be computed as follows:

$$
\begin{aligned}
\mu_{SCK} &= \int_{\Omega} \mathbf{Y^{SCK}}(\xi)W(\xi)\mathrm{d}\xi \\
&= \int_{\Omega} (\mathbf{Y^{SC}}(\xi) + \mathbf{Y^{Krig}}(\xi))W(\xi)\mathrm{d}\xi \\
&= \int_{\Omega} \mathbf{Y^{SC}}(\xi)W(\xi)d\xi + \int_{\Omega} \mathbf{Y^{Krig}}(\xi)W(\xi)\mathrm{d}\xi \\
&= \mu_{SC} + \mu_{Krig}
\end{aligned}
\tag{10}
$$

where μ_{SC} and μ_{Krig} are the mean of SC and Kr models. Hence, the mean of the stochastic process under study is the sum of the means of the SC and Kr models: both μ_{SC} and μ_{Krig} can be computed via the specific techniques available for standard SC and Kr modeling approaches (such as analytical, numerical integration or MC-based calculation).

The variance computation via SCK model is more complex. Indeed, Eq. (9) can be written as:

$$
\begin{aligned}
\sigma^2_{SCK} &= \int_{\Omega} (\mathbf{Y}(\xi) - \mu)^2 W(\xi)\mathrm{d}\xi \\
&= \int_{\Omega} (\mathbf{Y^{SC}}(\xi) + \mathbf{Y^{Krig}}(\xi) - \mu)^2 W(\xi)\mathrm{d}\xi \\
&= \int_{\Omega} (\mathbf{Y^{SC}}(\xi)^2 - 2\mu\mathbf{Y^{SC}}(\xi) + \mathbf{Y^{Krig}}(\xi)^2 - 2\mu\mathbf{Y^{Krig}}(\xi) \\
&\quad + \mu^2 + 2\mathbf{Y^{SC}}(\xi)\mathbf{Y^{Krig}}(\xi))W(\xi)\mathrm{d}\xi.
\end{aligned}
\tag{11}
$$

Using Eq. (10) and expanding, Eq. (11) is further simplified as:

$$
\sigma^2_{SCK} = \sigma^2_{SC} + \sigma^2_{Krig} - 2\mu_{SC}\mu_{Krig} + \gamma_{SCKrig}
\tag{12}
$$

where

$$
\gamma_{SCKrig} = 2 \int_{\Omega} (\mathbf{Y^{SC}}(\xi)\mathbf{Y^{Krig}}(\xi))W(\xi)\mathrm{d}\xi.
\tag{13}
$$

Hence, the variance of the stochastic process under study can be expressed via Eq. (12) and (13) as the sum of:

- a term σ^2_{SC} describing the variation of the global trend, which is exactly the variance of the SC model and it can be computed via any method available for standard SC modeling techniques.
- a term σ^2_{Krig} describing the variation of the local trend, which is exactly the variance of the Kr model and can be estimated accordingly.
- a term $2\mu_{SC}\mu_{Krig}$ which is the product of the means of the SC and Kr models.
- a term γ_{SCKrig} depending on the interaction of the SC and Kr model, which must be computed via numerical methods.

Note that if Eq. (13) is computed via numerical integration and the integrand is evaluated over the nodes chosen to build the SC model, then $\gamma_{SCKrig} = 0$: indeed, the Kr model is equal to zero in such nodes by construction (Sect. 4.2). For example, if the stochastic process depends on the Normal random variables and the Gauss points are used to compute the SC model, computing γ_{SCKrig} via numerical integration will give a non zero result only if the number of points used to estimate integral (13) is higher than the number of nodes used to compute the SC model.

It is evident from Eq. (10) that the proposed SCK approach preserves properties of SC and Kr in mean computation. Moreover, variance computation via Eq. (12) depends on the moments of SC and Kr models and an interaction integral which can be computed via numerical methods.

5 Numerical examples

5.1 Problem setup

Here, we demonstrate the performance of the proposed SCK approach for systems under the influence of uncertainty. The effectiveness of the new proposed ensemble technique (SCK) is compared with the state-of-art techniques Kr [8], SC [28], PC expansion [10], and PCK [14] on various problems. We consider two analytical

benchmark problems, while in the first case, we demonstrate the modeling capability of SCK and the second case shows the effectiveness in comparison to other approaches. Moreover, two practical engineering problems: a photonic directional coupler and a mechanical truss structure are considered in uncertainty analysis. In the following, we describe the specific settings adopted to build such models.

The SC technique for the numerical example considered is constructed over a Smolyak sparse grid based on the Clenshaw–Curtis and Gauss Legendre nodes [29], respectively. The Kr models have been computed via the open source ooDACE toolbox [44, 45]. The Gaussian correlation function given in Eq. (5) is used in all cases. The samples used to build the Kr models are generated via LHD sampling. Note that the proposed SCK method is based on the same setting adopted for the SC and Kr modeling techniques.

The PC expansion considered in the contribution is based on the least angle regression (LAR) algorithm and UQlab, a MATLAB UQ framework [46]. A more recently proposed Polynomial Chaos-Based Kriging (PCK) [14] modeling technique is used to compare the performance of the new proposed SCK method. It is a particular case of universal Kr, where a set of optimal orthogonal polynomials which are determined from LAR are used in the trend function of universal Kr. A complete discussion about the properties of PC and PCK is outside the scope of this contribution, but the interested reader can refer to [10, 11, 14, 37].

In the following section, various problems of dimensionality from two to ten and with different distributions of random variables are considered. The modeling power of all considered approaches is assessed by means of root-relative-squared-error measure (RRSE):

$$
\mathrm{RRSE} = \frac{\sum_{i=1}^{N} \left(\mathbf{Y}_i^{\mathrm{Exact}} - \mathbf{Y}_i \right)^2}{\sum_{i=1}^{N} \left(\mathbf{Y}_i^{\mathrm{Exact}} - E\left[\mathbf{Y}^{\mathrm{Exact}} \right] \right)^2}
\tag{14}
$$

where $\mathbf{Y}$ is the surrogate model response over N sample points and $E[\cdot]$ is the expectation of the output values $\mathbf{Y}^{\mathrm{Exact}}$, while the corresponding UQ is performed via MC analysis based on the selected surrogate modeling techniques.

5.2 Analytical benchmark functions

We considered two widely used analytical benchmark functions (Ackley [47, 48], and Sobol [49, 50]) of different dimensionality to describe in detail the calculation of an SCK model and to illustrate its modeling capabilities. In both the examples, the chosen random variables are considered independent and uniformly distributed.

5.2.1 Ackley function (2D)

The Ackley function is characterized by a global optimum and several local minimums. In a two-dimensional space, the random inputs are defined by their respective distributions $\{X_1, X_2\} \sim \mathrm{U}[-2, 2]$. It is expressed in terms of the random inputs as:

$$
f(\mathbf{x}) = -a\, exp\left(-b \sqrt{\frac{1}{2} \sum_{i=1}^{2} x_i{}^2} \right) - exp\left(\frac{1}{2} \sum_{i=1}^{2} \cos\left(c\, x_i \right) \right) + a + K
\tag{15}
$$

where $a = 20$, $b = 0.2$, and $c = 2\pi$, and $K = exp(1)$ are taken from [51]. For illustration purposes, a step by step landscape plots of building the SCK model is plotted. In Fig. 3a and b, the Ackley function and the SC model built on a sparse grid of level 4 are compared. It is important to note that the SC model captures the global trend easily; however, it fails to model the local variations (peaks and downs here) precisely with a low interpolation level. In Fig. 3c, such local variations (ΔY) are indicated by black dots and are easily captured by the Kr model built on the same set of data on which the residual error is computed (Fig. 3c). The final SCK plot is shown in Fig. 3d, which clearly resembles the Ackley function. Finally, in Fig. 4a and 4b, the performances of all five modeling approaches are compared on a RRSE scale: SCK offers a better accuracy than SC and PC and shows comparable RRSE with respect to Kr and PCK approaches.

5.2.2 Sobol function (8D)

In eight dimensions, the Sobol function is defined as follows:

$$
f(\mathbf{x}) = \prod_{i=1}^{8} \frac{|4\, x_i - 2| + c_i}{1 + c_i}
\tag{16}
$$

where the random variables are $\{X_1, \ldots, X_8\} \sim \mathrm{U}[0, 1]$, and c is considered [1, 2, 5, 10, 20, 50, 100, 500] from [50]. Since the number of parameters are relatively high, the problem is affected by the curse of dimensionality. For SC-based approaches, the efficient sparse grid construction in high dimensions also results in a rapid increase in the number of collocation points with respect to the increase in interpolation level, see Table 1. Fig. 5a, b shows the RRSE of the five different modeling approaches with respect to the number of samples used to build the corresponding model. Note that SCK outperforms both SC and Kr in terms of RRSE and sample size, as described in Fig. 5a, and shows comparable performance with respect to PC and PCK.
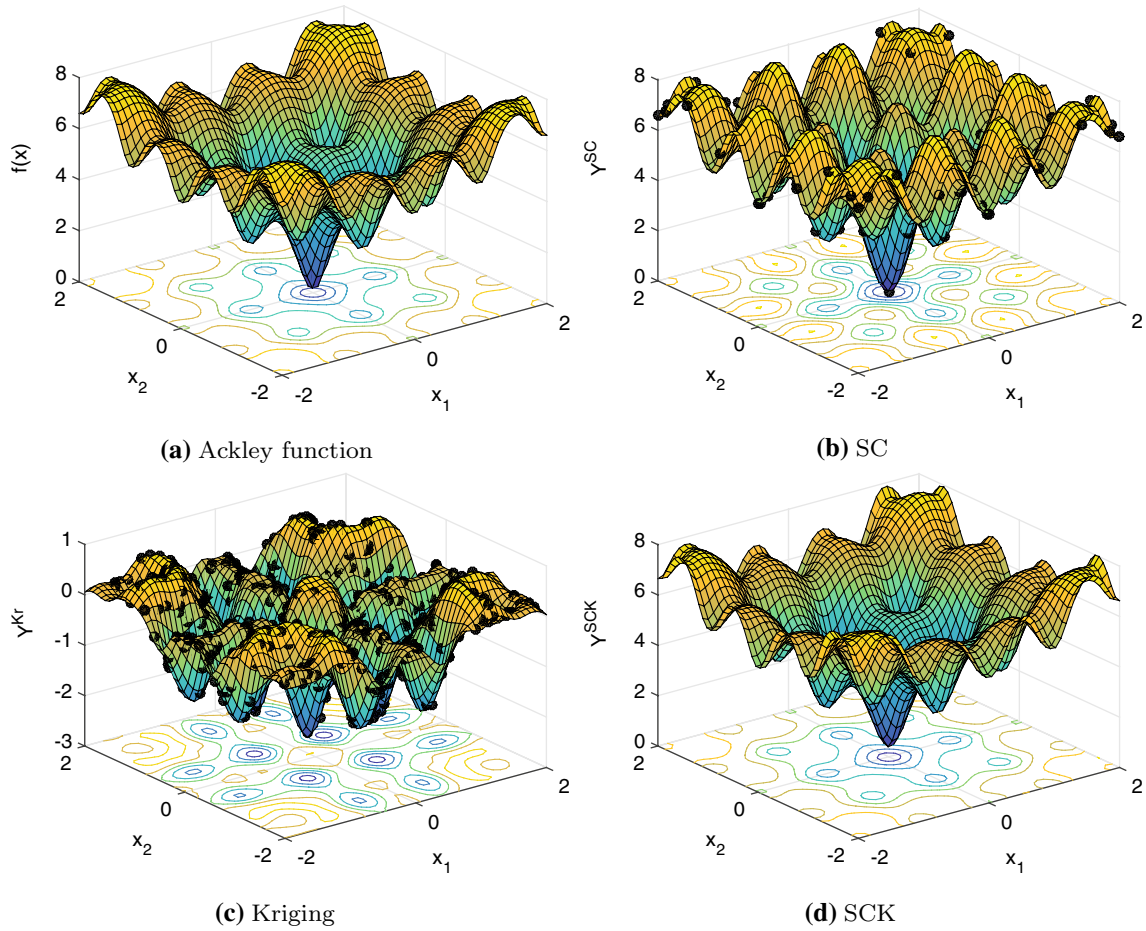
Fig. 3 **a** Ackley function, **b** SC model (level 4, 65 points), **c** Kr model built on 435 samples and residual error (ΔY) shown by *dots*, and **d** SCK model built on 500 samples
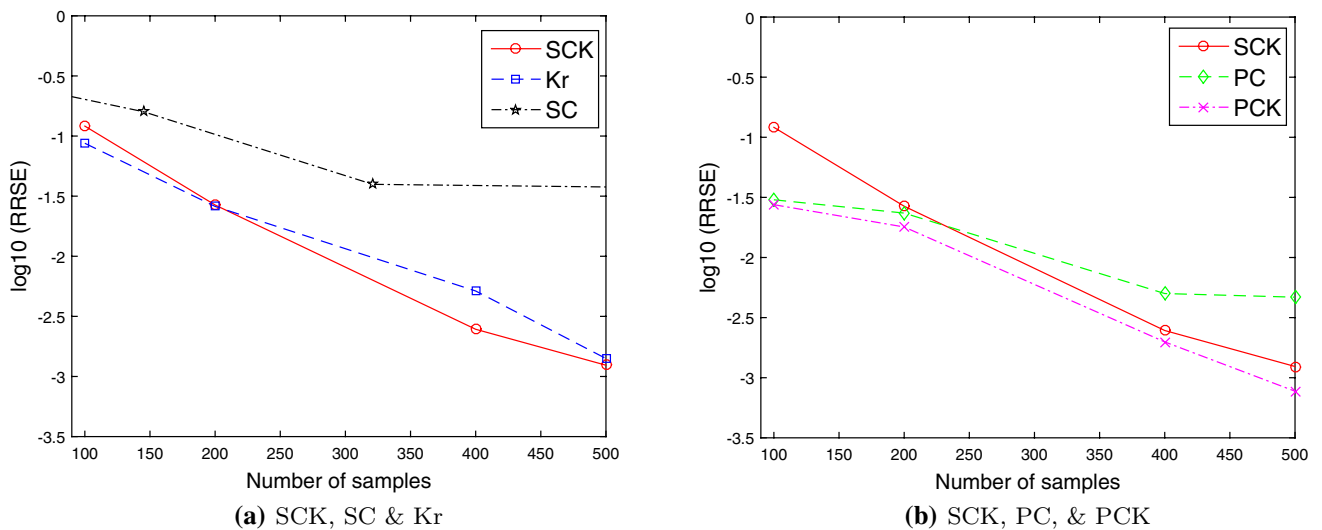

Fig. 4 RRSE plot for SC, Kr, PC, PCK, and SCK for the Ackley function
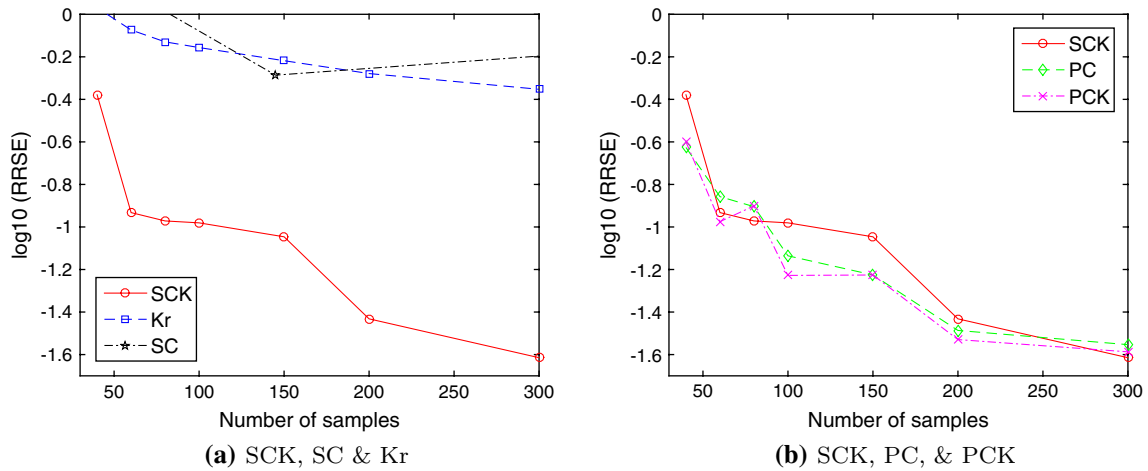
Fig. 5 RRSE plot for SC, Kr, PC, PCK, and SCK for the Sobol function
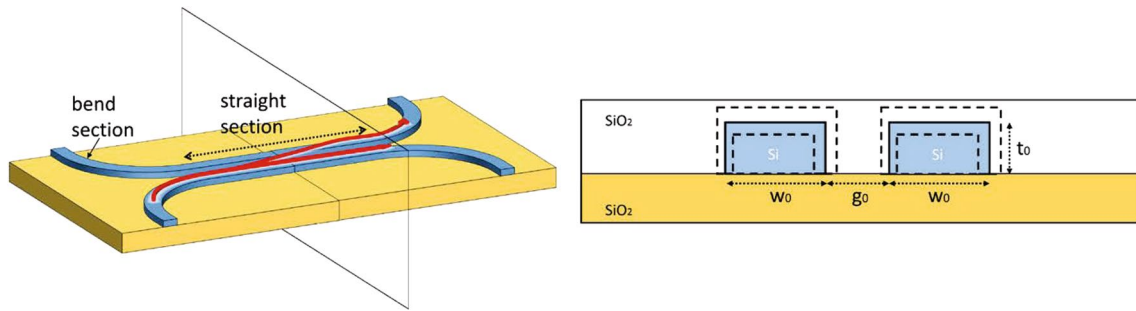

Fig. 6 *Left plot* perspective view of a symmetric DC [13], where the *Red arrows* indicates the flow of light. *Right plot* Amplified cross section. The mean width and thickness of the DC are w_o and t_o, respectively. The width w and thickness t of the fabricated DC are indicated as *dashed boxes*

5.3 Engineering applications

In this section, complex UQ problems of different engineering domains are studied. In the first example, we consider a 2D photonics problem (directional coupler) described in [13]. While, in the second case, a 10D mechanical truss structure [52] is studied for horizontal displacement at the free end.

5.3.1 Directional coupler (2D)

The proposed SCK modeling approach is applied to the UQ of a directional coupler (DC) in a silicon photonics platform [13] and shown in Fig. 6.

Precisely, the variance of the DC coupling coefficient κ is estimated with respect to the variability of the two geometrical parameters: the width w and thickness t of the DC are considered as the two correlated random variables following the Gaussian distribution. The nominal value of the width and thickness is considered as 450 and 220 nm, respectively, with normalized standard deviation of 2% with respect to their nominal value. It is assumed a correlation coefficient of 0.9 for the two random variables.

The proposed problem was studied in [13] only by means of the SC method, while here it is used to compare

Table 2 Performance summary of Kr, SC (levels 2 and 3), PC, PCK, and SCK

Algorithm	Number of samples	Mean	Percentage error (mean)	RRSE
Kr	25	65189	0.046	4.67×10^{-2}
SC (level 2)	13	65334	0.268	1.30×10^{-2}
SC (level 3)	29	65211	0.079	8.08×10^{-3}
PC	25	65121	0.058	1.48×10^{-2}
PCK	25	65165	0.009	2.96×10^{-3}
SCK	25	65149	0.015	9.85×10^{-4}

Note that the mean obtained by Fimmwave-based MC analysis is equal to 65159
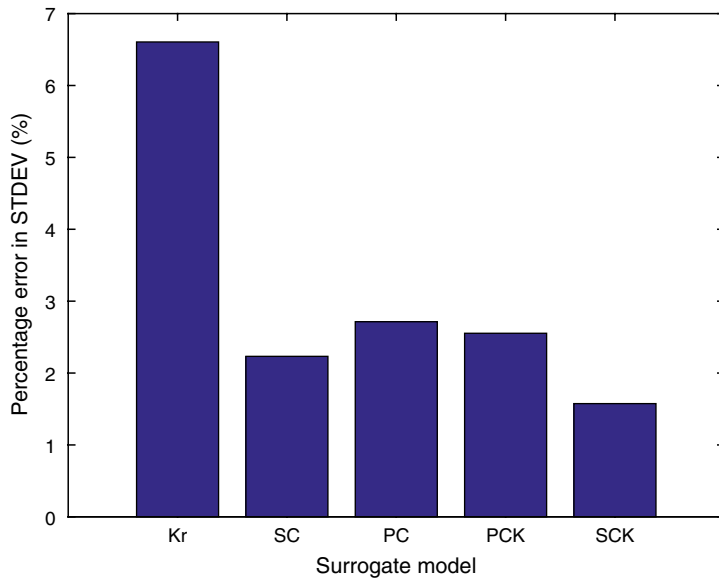
(a) Percentage error of the coupling coefficient STDEV.
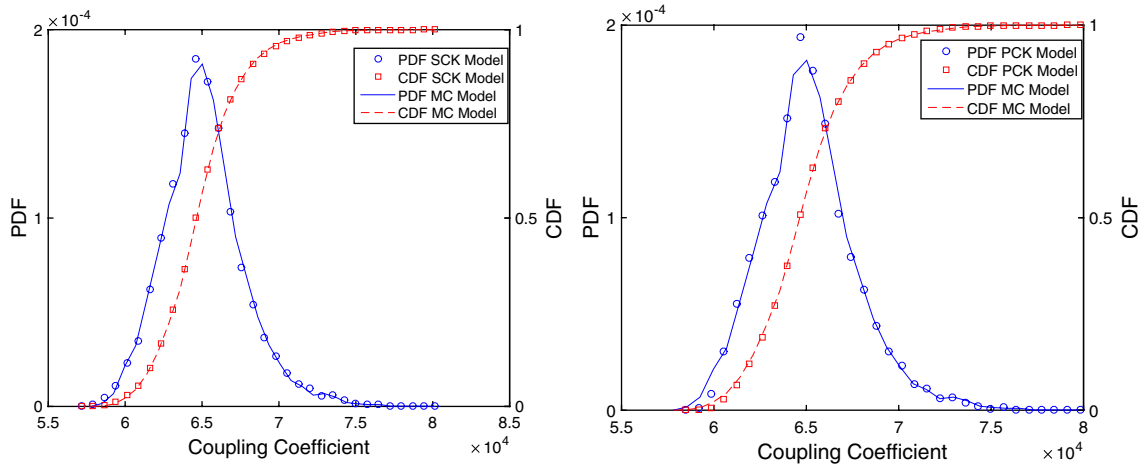
(b) SCK

(c) PCK
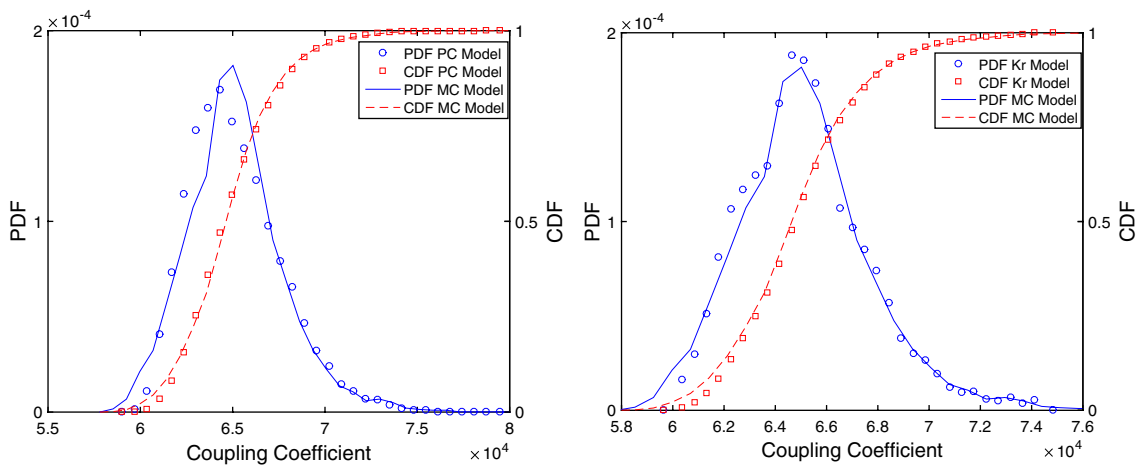
(d) PC

(e) Kr

Fig. 7 **a** Percentage error of the coupling coefficient STDEV and, **b–e** PDF and CDF of the coupling coefficient

Table 3 Total computational time (seconds) required to build and evaluate (10000 samples) each surrogate model

Algorithm	PC	Kr	SCK	SC	PCK
Number of samples (N)	25	25	25	29	25
Fimmwave solver (N) (s)	196.9	196.9	196.9	228.4	196.9
Model building (s)	3.55	3.61	2.49	0.09	4.25
Evaluation (s)	0.01	0.05	2.58	10.71	10.41
Total time (s)	200.4	200.5	201.9	239.2	211.5

Note that SC model is built with a level 3 sparse grid

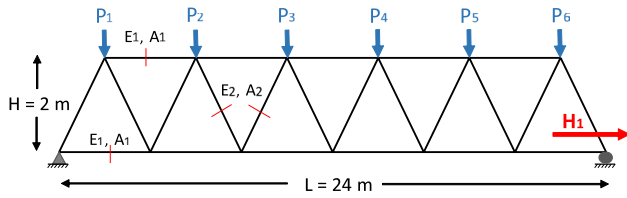**Fig. 8** Truss structure with 23 members

Table 4 Distribution parameters for input random variables

Variable	Distribution	Mean	STDEV
E_1, E_2 (Pa)	Lognormal	2.10×10^{11}	2.10×10^{10}
$A_1 (m^2)$	Lognormal	2.0×10^{-3}	2.0×10^{-3}
$A_2 (m^2)$	Lognormal	1.0×10^{-3}	1.0×10^{-4}
$P_1 - P_6$ (N)	Gumbel	5.0×10^4	10.0×10^3

Table 5 Performance summary of Kr, SC (levels 1 and 2), PC, PCK, and SCK

Algorithm	Number of samples	Mean	RRSE
Kr	150	18.437	5.90×10^{-3}
SC (level 1)	21	18.456	1.20×10^{-2}
SC (level 2)	261	18.459	6.19×10^{-5}
PC	150	18.458	2.57×10^{-3}
SCK	150	18.458	2.45×10^{-4}
PCK	150	18.454	2.37×10^{-4}

Note that mean obtained by MC analysis is equal to 18.459

performance of all five different techniques considered, namely Kr, SC, SCK, PC, and PCK. Note that the two random variables (w, t) are first de-correlated via a variable transformation using the Karhunen-Loéve expansion [53], then all the different modeling techniques considered are based on the independent Gaussian random variables obtained via such variable transformation. A

sample budget of 25 samples generated by LHS is used for all the selected approaches, with the exception of SC. Indeed, SC models are built over a pre-determined set of nodes chosen by means of the Smolyak algorithm (see Sect. 2 and Appendix 1): to describe the SC performance, two different sample sets consisting of 13 and 29 nodes are considered (corresponding to a Smolyak grid of level 2 and 3, respectively). A validation set of 10000 samples is used to compute the RRSE of all the approaches and to estimate statistical quantities via the MC analysis. Fimmwave, a commercially available software, is used to calculate the corresponding value of κ on a given geometry. The Fimmwave simulations have been performed on an Intel Core i5 2500 quad-core clocked at 3.3 GHz and 8 GB of memory.

The RRSE of all the modeling approaches is shown in Table 2. The proposed SCK method shows better modeling accuracy compared to Kr, SC, PC, and PCK. Moreover, the mean obtained by the five surrogate models for the coupling coefficient is reported in Table 2. Note that for the SC, SCK, PCK, and Kr model, the mean is obtained by MC simulation (10000 samples) on the constructed model, whereas in the case of the PC model, it is obtained analytically. From the results shown in Table 2, the mean value obtained by SCK is in excellent agreement with respect to the corresponding value obtained by the MC method, leading to a relative error of less than 0.01%.

Next, Fig. 7a presents the standard deviation (STDEV) of the coupling coefficient obtained via all five approaches. The percentage error is computed with respect to the reference MC value (STDEV = 2616.9). SCK gives best STDEV estimation when compared to other surrogate models. Note that the percentage error of the SC model built with 29 samples is shown in Fig. 7a. In addition, the PDF and CDF of κ obtained by SCK and MC are in good agreement, as shown in Fig. 7. Note that SCK offers the most accurate estimation of PDF and CDF when compared with the other surrogate models, see Fig. 7. The PDF and CDF of the SC method are not shown here, since the corresponding model was build on a different number of samples with respect to the other methods considered.

Furthermore, in Table 3, the computational cost of all selected approaches is compared. The total computational time is the sum of time required to build a model and MC simulations of the constructed model to estimate statistical moments (mean and standard deviation). Note that for the PC model, the statistical moments are computed analytically from the PC coefficients. The total computational time for SCK is 201.9s, which represents a speed-up of a factor 390× with respect to MC simulation which requires 21 h 53 min and 14 s to perform Fimmwave simulations on 10000 samples. Overall, computational cost of SCK is less
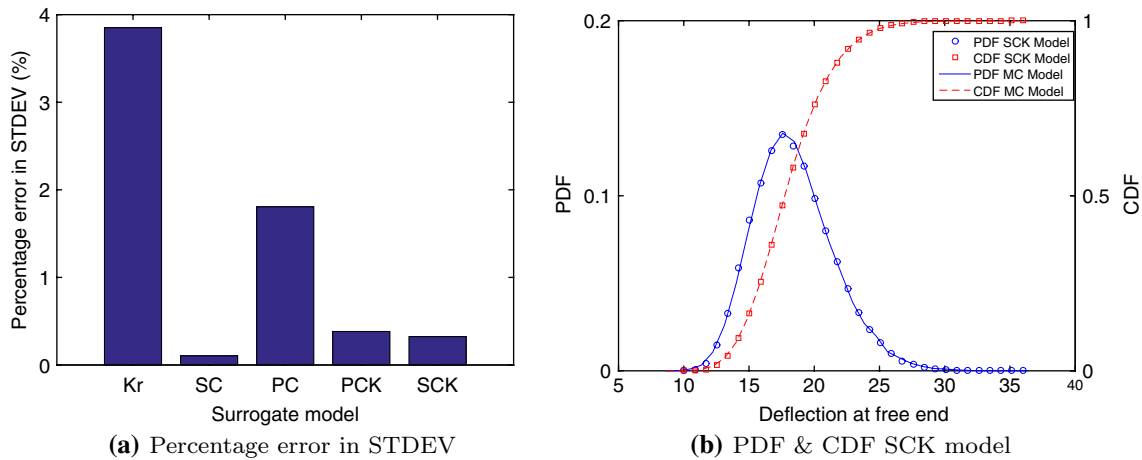
(a) Percentage error in STDEV

(b) PDF & CDF SCK model

Fig. 9 **a** presents the percentage error in estimating STDEV of the deflection at the free end by means of all five surrogate models. In **b**, the PDF and CDF of the deflection (in centimeter) at the free end are plotted

Table 6 Total computational time (seconds) required to build and evaluate (50000 samples) each surrogate model

Algorithm	PC	Kr	SCK	SC	PCK
Number of samples (N)	150	150	150	261	150
FE solver (N) (s)	0.41	0.41	0.41	0.71	0.41
Model building (s)	2.9	2.5	8.0	0.1	11.1
Evaluation (s)	1.0	132.0	404.0	1477.5	1938.2
Total time (s)	4.31	134.9	412.4	1478.3	1949.7

Note that SC model is built with a level 2 sparse grid

than SC and PCK, while it has a similar performance with respect to Kr and PC approaches.

5.3.2 Truss structure (10D)

In this example, we study a 2D truss structure as described in [52] for the displacement (H_1) of roller end in the horizontal direction. It is comprised of 23 horizontal and inclined members, as shown in Fig. 8. The truss structure is subjected to various point loads which are acting vertically on the nodes of the top frame.

Ten random variables are considered in the analysis, namely, the elastic modulus (E_1, E_2), the area of cross section (A_1, A_2) of the horizontal and diagonal truss elements, respectively, and the vertical point loads acting upon the top frame ($P_1, \ldots, P_6$). Such variables are assumed as independent following the distributions in Table 4. The complete structure is analyzed by a finite-element model comprised of 23 bar elements for the horizontal displacement at the free end by a finite-element program (FE) written in MATLAB. These simulations have been performed

on an Intel Core i5 4570 clocked at 3.2 GHz and 8 GB of memory.

A sample budget of $N = 150$ is used to construct surrogate models based on Kr, PC, PCK, and SCK. As for the previous example, two different SC models based on a level 1 ($N = 21$) and a level 2 ($N = 261$) Smolyak sparse grid are built. Table 5 describes the performance of the different modeling techniques. Note that the PCK and SCK models show the lowest RRSE error for the same sample size, while a level 2 SC model offers higher accuracy, but requires 74% more samples. Furthermore, all the modeling techniques are able to accurately estimate the mean value of the displacement at the free end, giving errors smaller than 0.1% with respect to the MC method (mean= 18.459). Moreover, as shown in Fig. 9a, STDEV computed by means of the SCK model is very accurate, with a relative percentage error of 0.33%, which is a significant improvement over SC (level 1) and the Kr models. Note that PCK and SCK show a percentage error of STDEV $< 0.39\%$ for the same sample budget. It is important to mention that the percentage error of the SC model built with 261 samples is shown in Fig. 9a. Finally, Fig. 9b shows the PDF and CDF of the displacement at the free end obtained by SCK and MC method, which are in excellent agreement.

The high modeling accuracy of PCK comes at the expense of relatively high computational cost, see Table 6. This is to be expected, since PCK is a particular case of universal Kr which relies on high order polynomial terms as a trend function: the model complexity increases with respect to the Kr approach considered. Note that with the increase in number of dimension, the number of polynomial terms increases rapidly in the trend function in PCK. Based on computational efficiency, SCK clearly outperforms PCK. In particular, Table 6 shows the total time required to built

each model and evaluate statistical moments. Note that the analysis of the truss structure under study is extremely fast to solve for displacement using a FE solver. As a result, MC simulations are very fast, and therefore, it is meaningless to compare the computational cost of selected methods with MC.

6 Conclusion

In modern engineering design, surrogate models are a valuable tool to carry out fast analysis of computation intensive processes. However, this leverage comes at the expense of a loss of accuracy. In this paper, a new modeling scheme is proposed based on SC and Kr. The proposed SCK algorithm is evaluated and compared over various benchmark and realistic problems with four different state-of-art techniques for surrogate modeling and uncertainty quantification, namely, SC, Kr, PC, and PCK. The proposed method clearly outperforms SC and Kr techniques and shows comparable performance with respect to the PC and recently proposed PCK modeling approach, especially when a high level of accuracy is required.

Appendix: Smolyak algorithm

The sparse interpolant $\mathbf{A}_{L,d}$ given by the Smolyak algorithm is [54]

$$\mathbf{A}_{L,d}(\xi) = \sum_{L-d+1 \leq |\mathbf{k}| \leq L} (-1)^{L-|\mathbf{k}|} \binom{d-1}{L-|\mathbf{k}|} \left(U^{k_1} \otimes \cdots \otimes U^{k_d}\right) \tag{17}$$

where $A_{L,d}$ is the weighted sum of d dimensional product rule, the vector $\mathbf{k}$ is formed by the interpolation level or order used for each variable, here $|\mathbf{k}| = k_1 + \cdots + k_d$, and L is the maximum level assumed for the sparse grid. In the above expression, the desired interpolant $\mathbf{A}_{L,d}$ is formed by combination of the one-dimensional rules U^{k_i} of order k_i which sum or total order $|\mathbf{k}|$ never exceeds the maximum level L.

To form an interpolant $\mathbf{A}_{L,d}$ in Eq. (17), the total number of points ($\mathbf{H}_{L,d}$) used by the interpolant is given by the following:

$$\mathbf{H}_{L,d} = \bigcup_{L-d+1 \leq |\mathbf{k}| \leq L} \Theta_1^{k_1} \times \cdots \times \Theta_d^{k_d} \tag{18}$$

where Θ denotes the set of points used in the one-dimensional function interpolation. Moreover, by choosing a suitable one-dimensional node scheme, e.g., Chebchev points, the set of collocation points Θ^k obtained are nested.

To illustrate the grid construction based on the tensor product and sparse grid, a two-dimensional example is used here. In particular, the Clenshaw–Curtis rule is adopted to choose the node for the interpolation in each dimension: the resulting collocation point is the extrema of the Chebyshev polynomials. The total number of points ($\mathbf{H}_{4,2}$) using a level 4 sparse grid is obtained by Eq. (18). As result, a maximum of 17 nodes are chosen for each dimension and a total of 65 collocation points (Fig. 10b) are required to build the desired SC model. The corresponding tensor product grid is obtained by the product of the 17 nodes chosen in each dimension by the Clenshaw–Curtis rule. As a result, 289 (17×17) points (Fig. 10a) are required to build the desired SC model by a tensor product, which is approximately 4.5 times the total number of points required by the corresponding sparse grid.
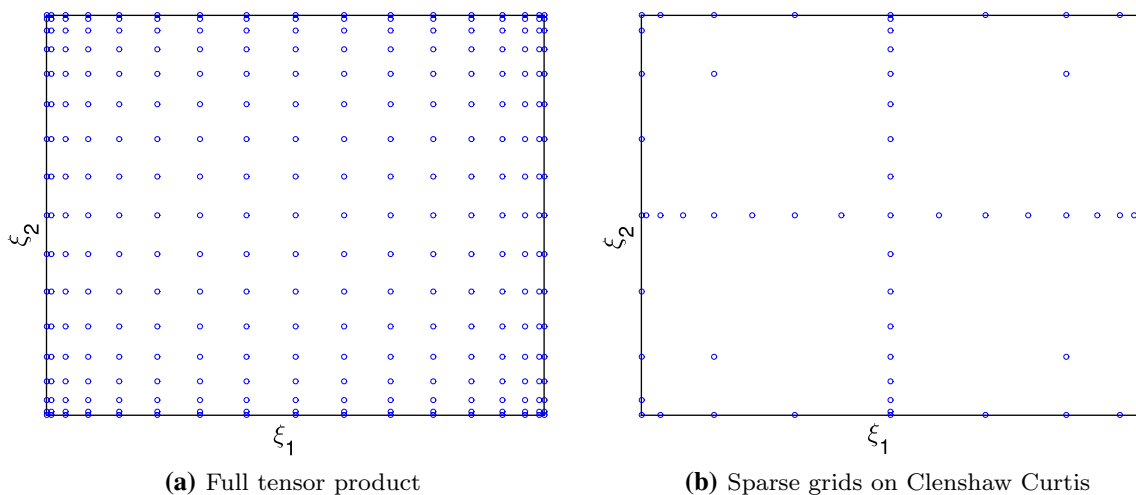

(a) Full tensor product

(b) Sparse grids on Clenshaw Curtis

Fig. 10 Two-dimensional tensor product based on 17 samples for each variable and corresponding Smolyak sparse grid $\mathbf{H}_{4,2}$ based on the Clenshaw Curtis rule

References

1. Gorissen D, Couckuyt I, Demeester P, Dhaene T, Crombecq K (2010) A surrogate modeling and adaptive sampling toolbox for computer based design. J Mach Learn Res 11:2051–2055

2. Jones DR, Schonlau M, Welch WJ (1998) Efficient global optimization of expensive black-box functions. J Global Optim 13(4):455–492

3. Wang G, Shan S (2007) Review of metamodeling techniques in support of engineering design optimization. J Mech Design 129(4):370–380

4. Witteveen J, Doostan A, Chantrasmi T, Pecnik R, Iaccarino G (2009) Comparison of stochastic collocation methods for uncertainty quantification of the transonic rae 2822 airfoil. Vrije Universiteit Brussel, Brussels, Belgium, Workshop on Quantification of CFD Uncertainties

5. Gorissen D, Couckuyt I, Laermans E, Dhaene T (2010) Multiobjective global surrogate modeling, dealing with the 5-percent problem. Eng Comput 26(1):81–98

6. Ganapathysubramanian B, Zabaras N (2007) Sparse grid collocation schemes for stochastic natural convection problems. J Comput Phys 225(1):652–685

7. Simpson T, Poplinski J, Koch PN, Allen J (2001) Metamodels for computer-based engineering design: survey and recommendations. Eng Comput 17(2):129–150

8. Sacks J, Welch WJ, Mitchell T, Wynn HP (1989) Design and analysis of computer experiments. Stat Sci 4(4):409–435

9. Dwight R, Han Z (2009) Efficient uncertainty quantification using gradient-enhanced kriging. In: Proceedings of the 11th AIAA non-deterministic approaches conference

10. Ghanem RG, Spanos PD ((1991)) stochastic finite elements: a spectral approach. Springer, New York, Inc., New York, NY, USA

11. Eldred MS ((2009)) Recent advances in non-intrusive polynomial chaos and stochastic collocation methods for uncertainty analysis and design. In: Proceedings of the 50th AIAA/ASME/ASCE/AHS/ASC Structures, Structural Dynamics, and Materials Conference, AIAA-2009-2274

12. Agarwal N, Aluru N (2011) Weighted smolyak algorithm for solution of stochastic differential equations on non-uniform probability measures. Int J Numer Methods Eng 85(11):1365–1389

13. Xing Y, Spina D, Li A, Dhaene T, Bogaerts W (2016) Stochastic collocation for device-level variability analysis in integrated photonics. Photon Res 4(2):93–100

14. Schöbi R, Sudret B, Wiart J (2015) Polynomial-based Kriging. Int J Uncertain Quantif 5(2):171–193

15. Clarke SM, Griebsch JH, Simpson TW (2004) Analysis of support vector regression for approximation of complex engineering analyses. J Mech Design 127(6):1077–1087

16. Han ZH, Görtz S (2012) Hierarchical kriging model for variable-fidelity surrogate modeling. AIAA J 50(9):1885–1896

17. Han Z, Zimmerman R, Görtz S (2012) Alternative cokriging method for variable-fidelity surrogate modeling. AIAA J 50(5):1205–1210

18. Wan X, Karniadakis GE (2005) An adaptive multi-element generalized polynomial chaos method for stochastic differential equations. J Comput Phys 209(2):617–642

19. Wan X, Karniadakis GE (2006) Multi-element generalized polynomial chaos for arbitrary probability measures. SIAM J Sci Comput 28(3):901–928

20. Witteveen JAS, Iaccarino G (2012) Simplex stochastic collocation with random sampling and extrapolation for nonhypercube probability spaces. SIAM J Sci Comput 34(2):A814–A838

21. Witteveen JAS, Iaccarino G (2012) Refinement criteria for simplex stochastic collocation with local extremum diminishing robustness. SIAM J Sci Comput 34(3):A1522–A1543

22. Matre OL, Najm H, Ghanem R, Knio O (2004) Multi-resolution analysis of wiener-type uncertainty propagation schemes. J Comput Phys 197(2):502–531

23. Matre OPL, Najm HN, Pbay PP, Ghanem RG, Knio OM (2007) Multi-resolution-analysis scheme for uncertainty quantification in chemical systems. SIAM J Sci Comput 29(2):864–889

24. Yang J, Faverjon B, Peters H, Kessissoglou N (2015) Application of polynomial chaos expansion and model order reduction for dynamic analysis of structures with uncertainties. Procedia IUTAM 13:63–70 (dynamical Analysis of Multibody Systems with Design Uncertainties)

25. Spina D, Ferranti F, Antonini G, Dhaene T, Knockaert L (2014) Efficient variability analysis of electromagnetic systems via polynomial chaos and model order reduction. IEEE Trans Compon Packag Manuf Technol 4(6):1038–1051

26. Blatman G, Sudret B (2011) Adaptive sparse polynomial chaos expansion based on least angle regression. J Comput Phys 230(6):2345–2367

27. Peng J, Hampton J, Doostan A (2014) A weighted ℓ_1-minimization approach for sparse polynomial chaos expansions. J Comput Phys 267:92–111

28. Preston JS, Tasdizen T, Terry CM, Cheung AK, Kirby RM (2008) Using the stochastic collocation method for the uncertainty quantification of drug concentration due to depot shape variability. IEEE Trans Bio-Med Eng 56(3):609–620

29. Barthelmann V, Novak E, Ritter Klaus (2000) High dimensional polynomial interpolation on sparse grids. Adv Comput Math 12(4):273–288

30. Gerstner T, Griebel M (2003) Dimension-adaptive tensor-product quadrature. Computing 71(1):65–87

31. Klimke A (2006) Uncertainty modeling using fuzzy arithmetic and sparse grids. PhD thesis, University Stuttgart, Shaker verleg, Aachen

32. Ma X, Zabaras N (2009) An adaptive hierarchical sparse grid collocation algorithm for the solution of stochastic differential equations. J Comput Phys 8:3084–3113

33. Ma X, Zabaras N (2010) An adaptive high-dimensional stochastic model representation technique for the solution of stochastic partial differential equations. J Comput Phys 229(10):3884–3915

34. Bungartz HJ, Griebel M (2004) Sparse grids. Acta Numerica 13:147–269

35. Griebel M (1998) Adaptive sparse grid multilevel methods for elliptic pdes based on finite differences. Computing 61(2):151–179

36. Bilionis I, Zabaras N (2012) Multi-output local gaussian process regression: applications to uncertainty quantification. J Comput Phys 231(17):5718–5746

37. Xiu D (2009) Fast numerical methods for stochastic computations: a review. Commun Comput Phys 5(2–4):242–272

38. Marrel A, Iooss B, Dorpe FV, Volkova E (2008) An efficient methodology for modeling complex computer codes with gaussian processes. Comput Stat Data Anal 52(10):4731–4744

39. Kleijnen JP (2009) Kriging metamodeling in simulation: A review. Eur J Oper Res 192(3):707–716

40. Sudjianto A, Chen W, Jin R (2002) On sequential sampling for global metamodeling in engineering design

41. Sasena MJ, Papalambros P, Goovaerts P (2002) Exploration of metamodeling sampling criteria for constrained global optimization. Eng Optim 34:263–278

42. Zhu Z, Zhang H (2006) Spatial sampling design under the infill asymptotic framework. Environmetrics 17(4):323–337

43. Stein ML (1999) Interpolation of the spatial data. Springer, New York

44. Couckuyt I, Dhaene T, Demeester P (2014) oodace toolbox: a flexible object-oriented kriging implementation. J Mach Learn Res 15(1):3183–3186
45. Couckuyt I, Forrester A, Gorissen D, Turck FD, Dhaene T (2012) Blind kriging: implementation and performance analysis. Adv Eng Softw 49:1–13
46. Marelli S, Sudret B (2014) UQLab: A Framework for Uncertainty Quantification in MATLAB. ETH-Zürich
47. Ackley DH (1987) A connectionist machine for genetic hill-climbing. Kluwer Academic Publishers, Norwell
48. Bäck T ((1996)) Evolutionary algorithms in theory and practice: evolution strategies, evolutionary programming, genetic algorithms. Oxford University Press, USA
49. Sobol I (2003) Theorems and examples on high dimensional model representation. Reliab Eng Syst Saf 79(2):187–193
50. Sudret B (2008) Global sensitivity analysis using polynomial chaos expansions. Reliab Eng Syst Saf 93(7):964–979 (bayesian Networks in Dependability)
51. Molga M, Smutnicki C (2005) Test functions for optimization needs. http://new.zsd.iiar.pwr.wroc.pl/files/docs/functions.pdf
52. Lee SH, Kwak BM (2006) Response surface augmented moment method for efficient reliability analysis. Struct Saf 28(3):261–272
53. Loeve M (1977) Probability theory, 4th edn. Springer, New York
54. Novak E, Ritter K (1999) Simple cubature formulas with high polynomial exactness. Constr Approx 15(4):499–522